NOCMAT 2026, v.1, e002

NOCMAT
https://periodicos.uefs.br/index.php/nocmat

ISSN
XXXX-XXXX

Effect of the sequence and mixing time of the alkaline solution on the synthesis of metakaolin-based geopolymers

Efeito da sequência e do tempo de mistura da solução alcalina na síntese de geopolímeros à base de metacaulim

AMORIM JÚNIOR, Nilson Santana[1]; ANDRADE NETO, José da Silva[2]; SANTANA, Henrique Almeida[3*]; CILLA, Marcelo Strozi[4]; RIBEIRO, Daniel Veras[5]

1 Department of Civil Construction, SENAI CIMATEC University. Salvador, Bahia, Brazil

2 Department of Architecture and Urbanism, State University of Santa Catarina, Laguna, Santa Catarina, Brazil.

3 Postgraduate Program in Civil and Environmental Engineering, State University of Feira de Santana, Feira de Santana, Bahia, Brazil.

4 Department of Materials Engineering, Federal University of São Carlos (UFSCar), São Carlos, São Paulo, Brazil.

5 Department of Materials Science and Technology (DCTM). Federal University of Bahia, Salvador, Bahia, Brazil

*Correspondent author: hasantana@uefs.br

Received: April 29, 2026
Accepted: August 07, 2026
Published: September, 1,2026

Citation: N. S. Amorim Júnior, J. S. Andrade Neto, H. A. Santana, M. S. Cilla, and D. V. Ribeiro, "Effect of the sequence and mixing time of the alkaline solution on the synthesis of metakaolin-based geopolymers," *NOCMAT*, vol. 1, e002, 2026. DOI.

Abstract
Geopolymers are alternative binders produced from aluminosilicate precursors activated by alkaline solutions. To improve practicality, one-part systems replace liquid activators with solid components, requiring only water addition. However, the influence of mixing sequence and activator maturation on geopolymerization remains unclear. This study evaluates geopolymeric matrices prepared using different mixing procedures, varying the preparation time of the alkaline solution and mixture type. Fresh-state behavior was assessed through flow tests (mini-V funnel and mini-slump), while hardened properties included shrinkage, compressive strength, and capillary absorption. Complementary analyses using calorimetry and FTIR were also performed. Results indicate that pre-mixing the precursor with the alkaline base accelerates geopolymerization but increases heat release, reducing workability and increasing shrinkage. Conversely, mixing with a matured alkaline solution at room temperature provided improved performance, balancing reactivity and workability. These findings highlight the importance of processing conditions in optimizing geopolymer systems.
***Keywords*:** geopolymer, mixing procedure, mortar, performance.

Resumo
Geopolímeros são ligantes alternativos produzidos a partir de precursores aluminosilicáticos ativados por soluções alcalinas. Para maior praticidade, sistemas “one-part” substituem ativadores líquidos por componentes sólidos, exigindo apenas adição de água. Contudo, a influência da sequência de mistura e da maturação do ativador na geopolimerização ainda não é clara. Este estudo avalia matrizes geopoliméricas preparadas por diferentes procedimentos, variando o tempo de preparo da solução alcalina e o tipo de mistura. No estado fresco, foram realizados ensaios de fluidez (mini funil V e mini slump); no estado endurecido, avaliaram-se retração, resistência à compressão e absorção capilar. Análises complementares por calorimetria e FTIR também foram conduzidas. Os resultados mostram que a pré-mistura do precursor com a base alcalina acelera a reação, mas aumenta o calor liberado, reduzindo a trabalhabilidade e elevando a retração. Já o uso de solução alcalina maturada proporcionou melhor desempenho geral.
Palavras-chave: geopolímero, procedimento de mistura, argamassa, desempenho.

1 INTRODUCTION

Geopolymeric matrices are produced through the activation of an aluminosilicate precursor with an alkaline activator, providing high mechanical performance and durability, which make them suitable as a substitute for Portland cement in several applications [1]. These binders can be synthesized from a wide range of raw materials, including metakaolin [1], fly ash [2], agro-industrial ashes [3], and red mud [4]. They have attracted considerable attention due to their lower CO_2 emissions compared with Portland cement [5–7]. However, their overall environmental benefit depends strongly on the type and dosage of the alkaline activator, since the production of activators, particularly sodium silicate, can contribute substantially to the total carbon footprint of the binder.

Generally, the preparation of geopolymers is the result of mixing a source of reactive aluminosilicates with an alkaline solution [5, 8]. The alkaline solution can be composed of sodium and/or potassium hydroxide and/or silicate [9-12], or a mixture of hydroxides and silicates [13-16]. During the reaction, aluminosilicates are dissolved, condensed, and polymerized, forming a gel with cementitious properties that leads to stiffening and strengthening [8, 17]. Depending on the physical state in which the alkaline activator is introduced into the mixture, and on the moment at which it comes into contact with the aluminosilicate precursor, geopolymer synthesis is generally classified into two distinct mixing methodologies: the two-part (or conventional) process and the one-part (or "just-add-water") process.

The two-part mixing process, described in the following sections, is widely used for practical applications. In this mixing process, the activating solution is prepared beforehand in its liquid form, typically an aqueous solution of hydroxide, silicate, or a combination of both, and only afterward is it mixed with the solid aluminosilicate precursor, as this is an extremely exothermic reaction [18]. Because the dissolution of hydroxide pellets and the interaction between hydroxide and silicate solutions release considerable heat, the activator solution is generally left to rest for a lead time that can vary between 3 and 24 h before mixing, allowing the solution to stabilize thermally and, in some cases, allowing further reorganization of the silicate species in solution. However, some researchers only expect the temperature of the solution to reach room temperature [19, 20], without any systematic studies on the impact of the advance time of preparation of the activator solution on the properties of geopolymers. Although widely used and generally associated with good mechanical performance, the two-part method presents practical drawbacks for large-scale applications, since it requires on-site handling of highly caustic liquid solutions, additional storage and mixing equipment, and strict control of the resting time and temperature of the activator prior to use.

In order to overcome these operational limitations and increase the commercial viability of the growing demands of geopolymer technology, recent research has produced geopolymers from a ready-mix precursor that can be mixed directly with water, similar to Portland cement [4, 18]. In this one-part mixture process, the solid activator (hydroxides, silicates, or others) is pre-blended in powder form together with the solid aluminosilicate precursor, so that a single dry mixture is obtained; only water is added at the time of producing the binder [21, 22]. This approach eliminates the need for preparing and handling a separate alkaline solution, simplifies transport and storage, reduces the exothermic effects associated with hydroxide dissolution during mixing, and allows the material to be used in a manner analogous to conventional cementitious binders, which is considered a key step toward the industrial-scale adoption of geopolymers.

While the one-part process offers clear practical and economic advantages, its relative mechanical performance compared to the two-part process remains a matter of debate. Nametollahi et al. [23] discovered that, even with these practical and economic advantages, one-part geopolymers had lower mechanical strength than that observed in two-part geopolymers (conventional mixing method). However, Peng et al. [24] obtained one-part geopolymers with superior mechanical performance compared to two-part geopolymers, demonstrating that a consensus does not exist on the most effective mixing method.

Beyond the choice between one-part and two-part processes, the mixing sequence and the order in which the raw materials and liquids are combined can also influence the fresh- and hardened-state properties of the resulting matrix. Dassekpo et al. [19] evaluated several mixing possibilities for geopolymer matrices based on fly ash. In the mixture that showed better synthesis and greater mechanical strength, the authors initially mixed dry materials (fly ash, sand, and sodium hydroxide) before adding the liquid solution, which was composed of sodium silicate, water, and superplasticizer additive.

Besides seeking matrices with better mechanical performance, the aim is to overcome one of the limitations of the consolidation of geopolymeric binders in real and large-scale applications by mastering the mixing procedure. Some authors [25, 26] emphasized the risk of handling activator solutions owing to the high alkalinity of geopolymer matrices during the mixing and application stages,

highlighting the need to standardize methods for production and handling of this material to make the practice safer.

Establishing clear criteria for choosing between one- and two-part mixing methods, and defining the most efficient mixing sequence for geopolymers primarily based on metakaolin, is a priority for advancing the practical consolidation of this technology and expanding its use in real, large-scale construction applications. Thus, this study evaluated the performance of geopolymeric mortars produced according to different mixing routines to verify whether the mixing procedure interferes with the properties in the fresh and hardened states.

One- and two-part procedures were analyzed along with the advance time for preparing the activating solution. In addition to rheological tests (mini-funnel V and mini-slump), evaluation of shrinkage, and physical-mechanical characterization (compressive strength and capillary suction), the efficiency of the mixing procedures was analyzed through calorimetry and Fourier transform infrared spectroscopy (FTIR) tests to evaluate the formation of phases.

2 EXPERIMENTAL PROCEDURE

2.1 MATERIALS

The materials used for the production of the geopolymeric mortars were HP Ultra metakaolin (Metacaulim do Brasil), sodium hydroxide (NaOH, 98% purity, O2 Científica), commercial sodium silicate solution (Na_2SiO_3, Exodus Científica), composed of 50 wt.% H_2O, 26.5 wt.% SiO_2, and 13.5 wt.% Na_2O, natural sand purchased from local suppliers, and distilled and deionized water.

2.2 METHODS

2.2.1 Materials Characterization

The physicochemical characterization of metakaolin was based on particle size distribution (Cilas 1180 laser granulometer), specific surface area (Gemini VII, Micromeritics), specific gravity by helium gas pycnometry (AccuPyc II 1340, Micromeritics), and chemical composition by X-ray fluorescence (S2 Ranger, Bruker). Particle size distribution was determined by laser diffraction using deionized water as the dispersing medium. The particle size distribution was calculated based on Mie scattering theory. At least three measurements were performed, and the reported results correspond to the average values. The BET specific surface area was determined by nitrogen adsorption at 77 K after degassing the samples under vacuum at 105 °C for 12 h. Specific gravity measurements were performed using helium gas, and chemical composition was expressed as oxide contents.

The metakaolin was mineralogically characterized by X-ray diffraction (XRD) using a Bruker D2 Phaser X-ray diffractometer equipped with a Cu Kα radiation source ($\lambda = 0.15406$ nm), operated at 30 kV and 10 mA without a secondary monochromator. Powder samples were mounted in PMMA sample rings (Ø 51.5 mm, height 8.5 mm), and their surfaces were carefully leveled to minimize preferred orientation effects. Diffraction patterns were collected over a 2θ range from 5° to 80°, using a step size of 0.02°, with a total acquisition time of approximately 1 h. Mineralogical phases were identified using the Diffrac.EVA software package and the Crystallography Open Database (COD). Phase quantification was performed by Rietveld refinement using Bruker's TOPAS software and Crystallographic Information Files (CIFs).

The specific gravity of the sand was determined using the proceedings of NBR 16916 [27]. The maximum characteristic size, average diameter (D_{50}), and fineness module (FM) were determined using the NBR 17054 [28] procedure.

2.2.2 Mixing Procedures

As shown in Figure 1, five mixing protocols were defined to verify the influence of mixing sequence on the formation of phases in pastes and on the properties of mortars in the fresh and hardened states. Each protocol is detailed below, in which pastes and mortars differ by the presence of sand and by the method of mixing:

- M1 - Sodium hydroxide mixed with metakaolin and sand, with subsequent addition of sodium silicate solution (SSS), at the time of mixing (one-part system).
- M2 - Sodium hydroxide and sodium silicate solutions prepared and mixed with metakaolin and sand, at the time of mixing (two-part system).
- M3 - Sodium hydroxide solutions prepared 24 hours in advance and subsequently mixed with SSS, metakaolin, and sand (two-part system);
- M4 – Sodium hydroxide solution prepared 24 hours in advance, mixed with the SSS 3 hours in advance, and added to the metakaolin and sand at the time of molding (two-part system).
- M5 – Sodium hydroxide and sodium silicate solutions prepared and mixed 24 h in advance; the resulting activating solution was then added to the metakaolin and sand at the time of molding (two-part system).

The paste composition was defined on a mass basis as 1:0.5:0.75 (metakaolin hydroxide solution silicate solution). Meanwhile, for the mortar it was 1:2:0.5:0.75 (metakaolin : sand : sodium hydroxide solution : sodium silicate solution, by mass) for all mixing routines. This formulation was based on Lizcano et al. [29], in accordance with the ranges recommended by Davidovits [10] to obtain the geopolymeric binder. The pastes were manually mixed for 60 s. The mortars were produced in a planetary bench mixer with a capacity of 5 L at low speed (62.5 ± 5.0 rpm) for 4 min.

Figure 1: Schematic of the mixing procedures adopted.

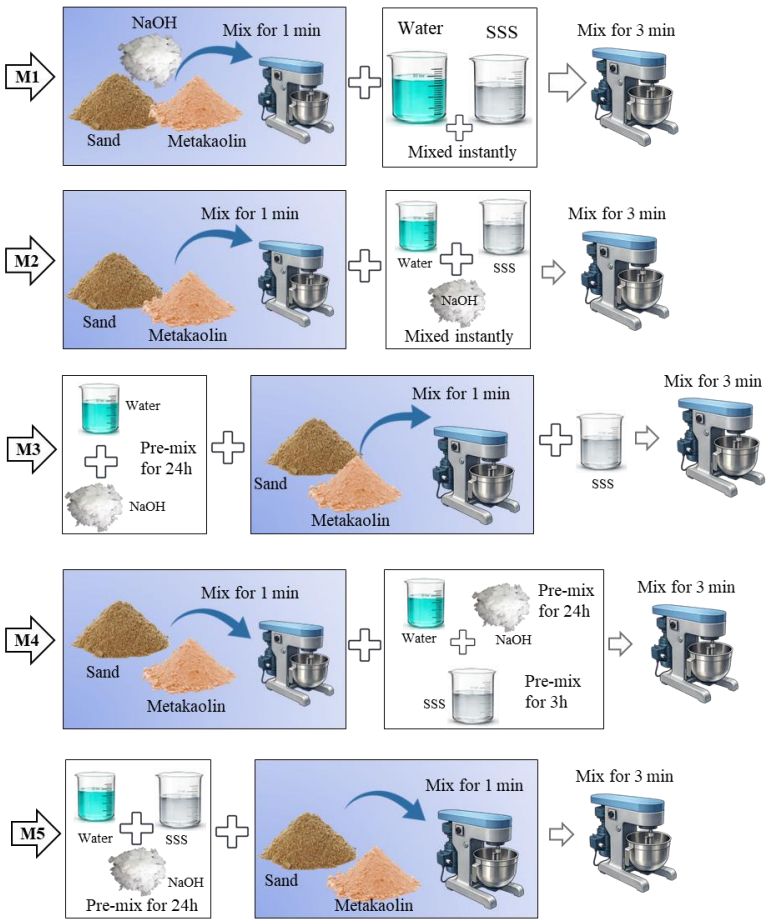

2.2.3 Evaluation of the pastes

The evolution of the heat released by the pastes was monitored using a four-channel isothermal calorimeter (Calmetrix, model 4000 HPC). The pastes were prepared following the same mixing procedures adopted for the corresponding mortars under each mixing routine, with the only difference being the omission of sand from the formulations. Immediately after mixing, approximately 60 g of paste were transferred to the Teflon sample cup of the calorimeter. A reference with an equivalent heat capacity, supplied by the manufacturer, was placed in the reference cell. The heat flow (mW/g of paste) and cumulative heat (J/g of paste) were continuously recorded during the first 70 h of reaction under isothermal conditions at 20 °C.

The phase formation of the geopolymeric pastes was investigated by Fourier-transform infrared spectroscopy (FTIR) using a Shimadzu PRESTIGE-21 spectrometer. After casting, the specimens were stored in air at 23 °C under the same conditions adopted for all other experimental tests until the age of 28 days. On the day of testing, representative fragments were collected and manually ground in an agate mortar. The resulting powder was sieved through a 75 μm mesh, and the passing fraction was immediately mixed with infrared-grade potassium bromide (KBr) to minimize further atmospheric carbonation and moisture uptake before being mechanically pressed into pellets for analysis. Prior to testing, a background ("blank") spectrum was collected in the absence of the sample to eliminate contributions from atmospheric species, particularly CO_2 and water vapor. Sixteen scans were acquired over the wavenumber range of 400–4000 cm^{-1}.

2.2.4 Tests on fresh mortars (Mini-funnel V and mini-slump)

The evaluation of the flow parameters of the mixtures in the fresh state was performed using mini-slump and mini-funnel V tests (Figure 2), following the procedures and dimensions of the apparatus described by EFNARC [30, 31]. In the mini-funnel V test, the flow time (t_{flow}) necessary for a 1.1-liter volume of mortar (funnel capacity) to flow through the bottom of the funnel was measured in seconds. Subsequently, the mini-slump test was performed to determine the measures of the spreading diameter (D_{spr}) of the molded mortar from the action of its own weight using a cone with 100 mm diameter at the base, 70 mm diameter at the top, and a 60 mm height.

Figure 2: Tests to determine the flow parameters: (a) mini-slump and (b) mini-funnel V.

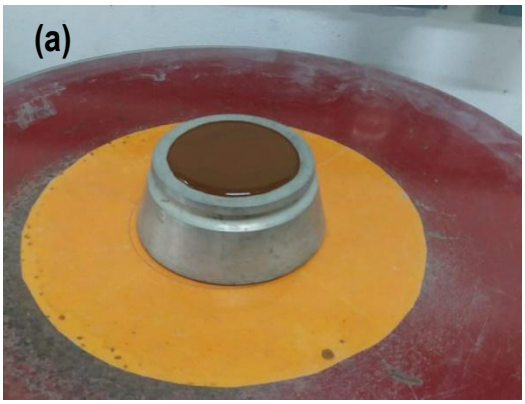

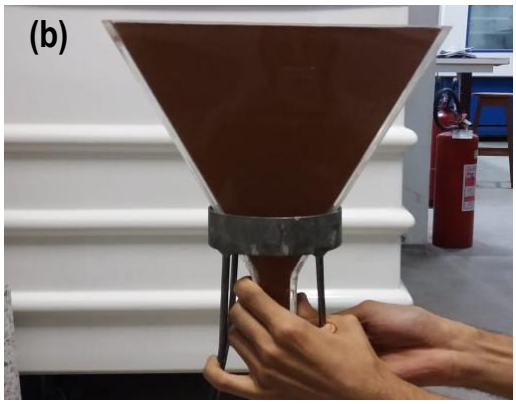

2.2.5 Molding and preparation of specimens

In total, eight prismatic specimens (40 mm × 40 mm × 160 mm) were molded for each routine used to determine the physical-mechanical properties of the mortars. The specimens were molded according to the recommendations of NBR 5738 [32] and cured by wrapping the specimen in plastic film after 24 h of molding and subsequent conditioning in an oven at 60°C, where they remained for a period of 24 h, then removed and cured in air (approximately 23°C) until the age of testing.

2.2.6 Tests of hardened mortars

The shrinkage test was conducted following the guidelines of ASTM C157/C157M (Standard Test Method for Length Change of Hardened Hydraulic-Cement Mortar and Concrete). Three prismatic specimens (25 mm × 25 mm × 285 mm) were prepared for each mixture. The specimens were demolded 24 h after casting, and their initial lengths were measured using an extensometer with an accuracy of 0.001 mm. Subsequently, the length change of each specimen was monitored daily for 38 days to evaluate the shrinkage behavior.

The capillary absorption coefficients or sorptivity of the three specimens of each mixing routine were determined according to the procedure described in NBR 9779 [33]. After 28 days of curing, the specimens were dried in an oven at 105°C and placed vertically on supports in a water layer 5 mm above its lower face.

The weight of the specimen was monitored in a time period throughout the contact with water (3, 6, 24, 48, and 72 hours). Sorptivity (S) refers to the volume of water penetrating per unit area and time ($kg/m^2.min^{0.5}$) which was calculated to facilitate the interpretation of the results. and was obtained empirically from the slope of the cumulative volume of water absorbed per unit area of inflow surface versus the square root of time, as represented in Eq. 1.

$$V_w / A_c = S.\sqrt{t} + S_o \quad (1)$$

where V_w denotes the mass of water absorbed (kg), A_c represents the cross-sectional area of each specimen (m^2), and t denotes the exposure time (min).

The axial compressive strength of the mortars obtained with different mixing routines at 3, 7, and 28 days were determined according to the guidelines of NBR 5739 [34]. The tests were performed on a servo-hydraulic testing machine with a model HD-120T, having a maximum capacity of 120 kN, and a tension increase rate of 0.45 MPa/s.

3 RESULTS

3.1 MATERIAL CHARACTERIZATION

Table 1 lists the physical characterization of the metakaolin and sand used in the analysis. Metakaolin has a high specific area and a small median equivalent particle diameter (D50). The parameters are typical for this type of material and suitable for good reactivity, which is desirable for materials used as geopolymeric precursors [6, 35].

Table 1: Physical characterization of the materials used.

Characteristic	Metakaolin	Sand
Average equivalent diameter of the particle (D_{50}) (μm)	8.0	0.36
Specific gravity (g/cm^3)	2.71	2.65
Specific Surface Area BET (m^2/g)	12.02	-
Fineness module	-	1.75
Maximum characteristic dimension (mm)	-	1.18

The chemical composition of metakaolin, determined by X-ray fluorescence (XRF), is listed in Table 2. As expected, metakaolin has the majority composition of SiO_2 and Al_2O_3. Figure 3 illustrates the X-ray diffractograms of metakaolin, with the identification and quantification of its crystalline phases.

Table 2: Chemical compositions, in oxides, of metakaolin (% by mass), obtained by XRF.

Materials	SiO_2	Al_2O_3	Fe_2O_3	K_2O	MgO	SO_3	CaO	TiO_2	OTHERS	LOI*
Metakaolin	50.12	40.03	2.40	2.43	1.53	0.07	0.08	1.66	0.33	1.40

*LOI = loss on ignition determined by heating the samples in a muffle furnace at 1000 °C.

Figure 3: X-ray diffractograms of metakaolin, with identification and quantification of crystalline phases and amorphous phase content.

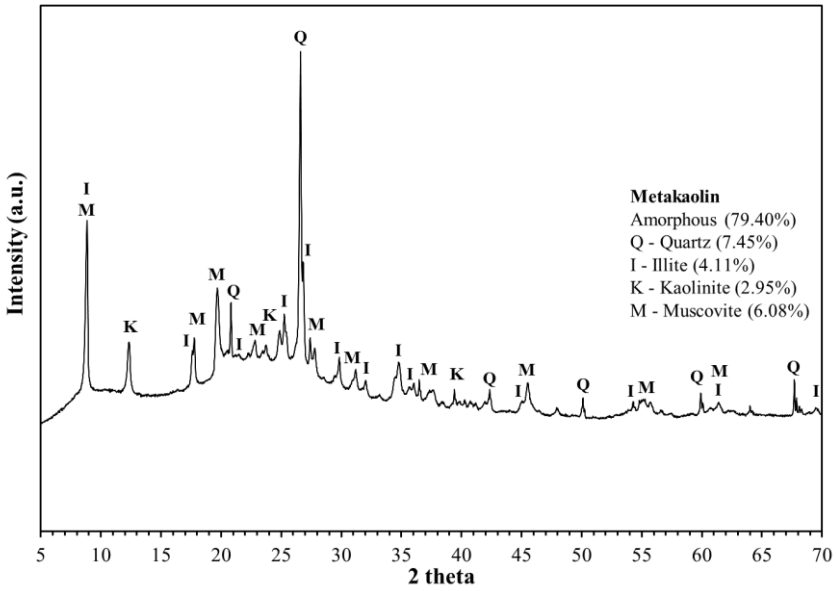

Typical crystalline phases of metakaolin, such as quartz (SiO_2), were identified, including muscovite [$KAl_2(Si_3Al)O_{10}(OH,F)_2$], kaolinite ($Al_2O_3.2SiO_2.2H_2O$), and illite ($Al_2H_2KO_{12}Si_4$), indicating partial dehydroxylation of metakaolin. The content of amorphous phases found in the sample was 79.40%, which is favorable to the geopolymerization process, as the amorphous phases of silica and alumina effectively dissolve during the reaction [36].

3.2 EVALUATION OF THE PASTES

3.2.1 Isothermal calorimetry

Figure 4A illustrates the accumulated heat result, obtained by isothermal calorimetry, for the pastes produced with different mixing procedures, with emphasis on the first 10 h of testing (Figure 4B).

It was observed that in the first hour, mixture 2 (M2) exhibited greater heat release. The behavior is attributable to the dissolution of the highly exothermic sodium hydroxide solution prepared during mixing. Mixture 1 (one-part) presented a heat release that is slightly lower than that of mixture M2, because the sodium hydroxide, still solid, was dispersed in the metakaolin, interfering with the dissolution kinetics. The result is owing to the fact that the metakaolin particles prevented a portion of water from being available to the NaOH particles, causing, in the initial moments, the accumulated heat released by the M1 mixture to be lower than the M2 mixture. Mixtures M3, M4, and M5 released a lower amount of heat in the first hours, as the solutions were at room temperature at the time of mixing. After approximately 24 h of testing, the M1 mixture began releasing more heat than M2, demonstrating that the reaction for this procedure had a longer duration. This phenomenon can be explained by the lower dissolution kinetics of the reaction. More specifically, water was gradually made available to the NaOH particles due to the interference of metakaolin particles.

The M3 mixture exhibited higher heat release than the M4 and M5 mixtures, possibly owing to the sodium silicate and sodium hydroxide solution prepared at the time of the M3 mixture. It triggered a

more intense exothermic reaction than that observed in the M4 and M5 mixtures, in which the Na_2SiO_3 and NaOH solutions were prepared 3 h and 24 h before mixing, respectively, at room temperature. Lastly, there is also a tendency to stabilize the heat released by the mixtures M2, M3, M4, and M5, which presented similar values of total accumulated heat at the end of the test.

Figure 4: (A) Comparison of accumulated heat for pastes produced with different mixing procedures and (B) highlight for the first 10 hours of testing.

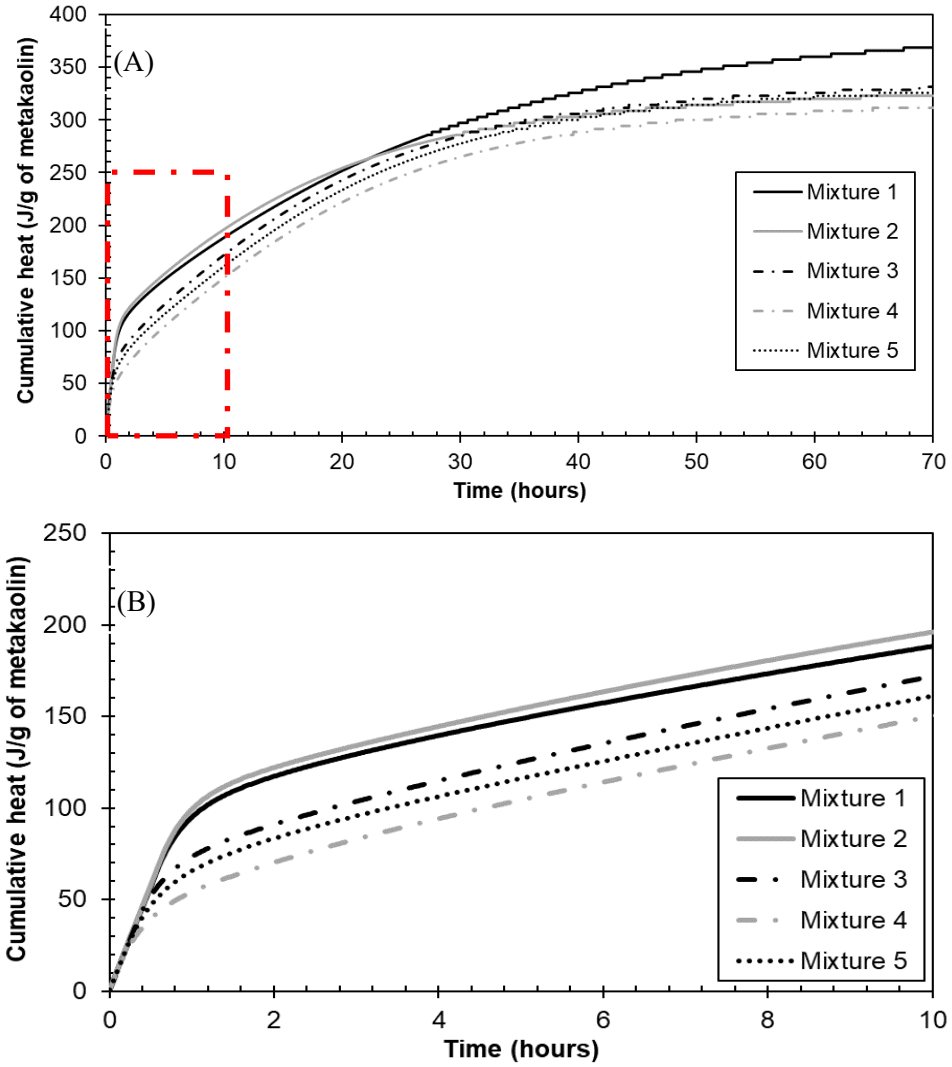

According to Ling et al. [37], two large exothermic peaks were observed in the geopolymer calorimetric curve. The first is the result of precursor dissolution in silicate and aluminate monomers, which is known as the dissolution peak. At the second peak, known as the polymerization peak, the silicate and aluminate monomers begin to polymerize into aluminosilicate oligomers and produce geopolymeric fragments, which is essential for the development of geopolymer strength. Thus, the greater the accumulated heat, the greater the formation of geopolymerization products [38], which indicates that mixtures M1 and M2 presented more intense reactions, with greater formation of geopolymerization products.

The result indicates that the pastes prepared with routines M1 and M2 possibly have the lowest setting times. Thus, depending on the geopolymer formulation, one-part procedures can result in a short setting time, or even a flash-set, which would make most practical applications of this material unfeasible.
The results obtained in this research exhibited the same pattern observed by HU et al. [39], who produced geopolymers with fly ash and using Na_2SiO_3 and NaOH as alkaline activators.

3.2.2 Phase formation analysis (FTIR)

Figure 5 illustrates the FTIR analysis of the matrices obtained from the five mixing routines evaluated. Five well-defined bands can be observed. The first (1) and second (2) bands refer to wave numbers 3440 cm^{-1} and 1640 cm^{-1}, respectively, indicating the elongation vibrations of the O-H and H-O-H bonds of the adsorbed water molecules [40-42]. The third band (3), corresponding to the wave number 1420 cm^{-1}, indicates the elongation of C-O-C vibrations, confirming the presence of carboxylic groups [41, 43]. The fourth band (4), located at approximately the wave number 1020 cm^{-1}, which indicates vibrations between the (Si,Al)-O-Si bonds [44]. The last band (5), at approximately 460 cm^{-1}, is formed due to vibrations in the Si-O-Si bonds [42, 43].

Figure 5: Fourier transform infrared spectroscopy (FTIR) analysis for the evaluated mixtures.

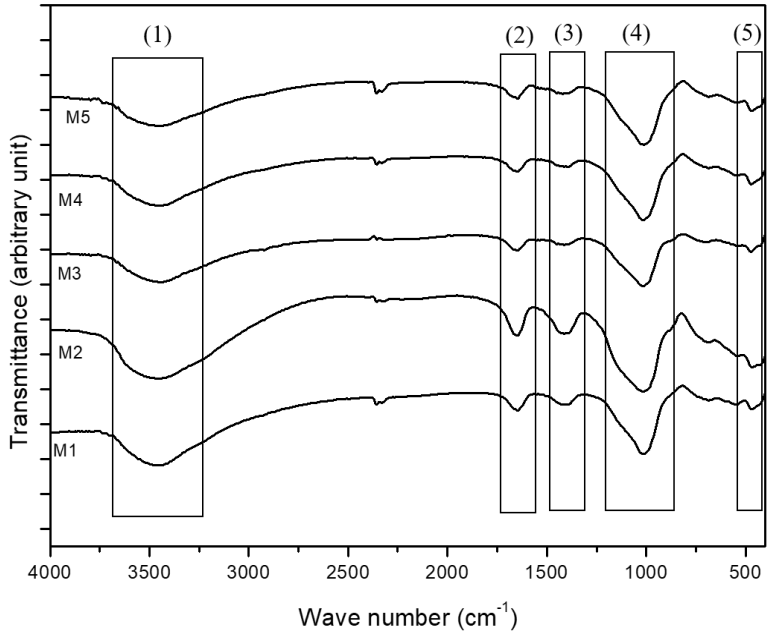

Notably, M1 and M2 mortars presented greater band intensity in the first region, and M2 also exhibited greater band intensity in the second and fourth regions. The first two bands indicate the water molecules present in the N-A-S-H gel [42] and the formation of the aluminosilicate network in a polymeric structure [45]. Overall, these results point to a greater synthesis of geopolymerization of the M1 and M2 mixtures, converging with the greatest accumulated heat observed for these mixtures. Moreover, the fourth band, which is more intense for M2, represents a greater dissolution and formation of the geopolymer gel [46].

The third band is associated with the elongation vibrations of C−O−C in carbonate components (CO_3^{2-}), indicating the presence of sodium carbonate (Na_2CO_3) in the matrix [42, 47], which is indicative of excess free and unreacted sodium [48]. However, usually, sodium carbonate manifests as efflorescence on the surface of specimens, a phenomenon that was not identified in the samples analyzed. It is possible that the amount of sodium carbonate formed was insufficient to form efflorescence on the surface of the specimen, remaining only in the matrix pores. The last band, which, according to Kumar and Kumar [41], corresponding to the dissolution of silicates, did not exhibit a shift in wave number or a significant increase in intensity for the studied mortars, regardless of the adopted mixing routine.

3.3 TESTS OF MORTARS IN THE FRESH STATE (MINI-FUNNEL V AND MINI-SLUMP)

Figure 6 illustrates the mortar flow time values in the mini-funnel V test for the five mixtures analyzed.

It was observed that the M1 and M2 mixtures had a shorter flow time, possibly owing to greater heat release (based on the results of isothermal calorimetry), which accelerates the metakaolin dissolution

and, consequently, reducing the viscosity. It should be mentioned that this test took place approximately 3 min after mixing the mortars; thus, the effect of the heat released in the mixture contributed little to the evaporation of water.

Figure 6: Mortar flow time after mini-funnel V test, in seconds.

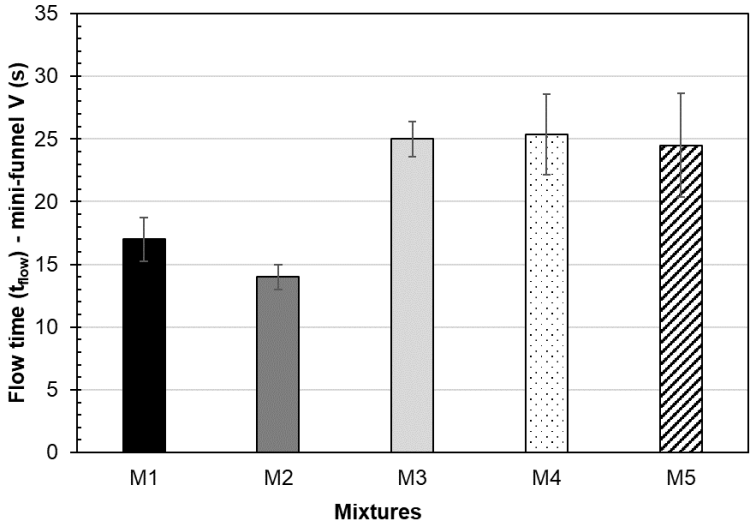

Figure 7 illustrates the spreading diameter values in the mini-slump test, whose results are associated with the yield strength, for the five mortar mixtures analyzed.

Figure 7: Spreading (opening diameter) of mortars after mini-slump test, in mm.

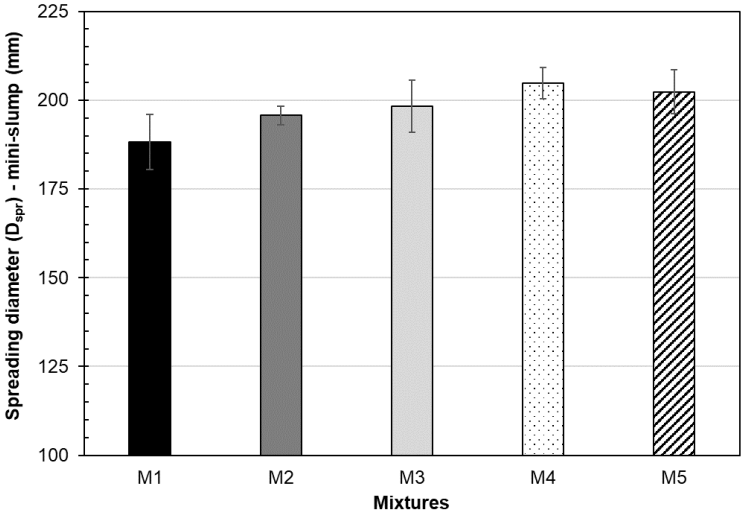

The M1 mixture exhibited the lowest spreading diameter, whereas M2 showed intermediate values that were not statistically different from the other mixtures. This behavior contrasts with that observed in the mini V-funnel test. The lower spread observed for M1 is likely associated with the greater heat release measured by isothermal calorimetry. The increase in temperature accelerates metakaolin dissolution and, consequently, the geopolymerization reactions [38,39], promoting the formation of aluminosilicate gel and increasing the yield stress of the fresh mixture. As a result, the precipitation of geopolymerization products at the time of the mini-slump test may have restricted the flowability of M1, leading to a lower spreading diameter.

According to the one-way ANOVA (Table 3), significant differences were observed among the mixtures ($p < 0.05$). However, Tukey's post hoc test revealed that only M1 presented a significantly lower spreading diameter than M4 and M5, whereas no statistically significant differences were found among

M2, M3, M4, and M5. Furthermore, no significant effect was observed when comparing mortars produced with alkaline solutions prepared before mixing at room temperature.

Table 3: Statistical reliability for the mini-slump test, through analysis of variance (ANOVA).

Mini-Slump	SQ	GL	MQ	F	p value	Fc	Significant Effect
M1-M5[1]	1121.80	4.00	280.45	3.93	0.04	3.63	Yes
M1-M5[2]	641.63	9.00	71.29				
M3-M5[1]	94.17	2.00	47.09	0.67	0.55	5.14	No
M3-M5[2]	420.96	6.00	70.16				

Note: SQ – Square sum; GL – Degrees of freedom; MQ – square average; F – Calculated value of F; p value – significance level; Fc – F critical; If p < 5% and Fc < F, the effect is significant, considering the 95% confidence interval.

[1] Between Groups; [2] Within groups.

3.4 TESTS OF MORTARS IN THE HARDENED STATE

3.4.1 Sorptivity

Figure 8 illustrates the sorptivity values for the different mixtures studied after 28 days. There is a distinction between the sorptivity of the M1 and M2 mixtures and of the M3, M4, and M5 mixtures.

Figure 8: Sorptivity for different mortar mixtures.

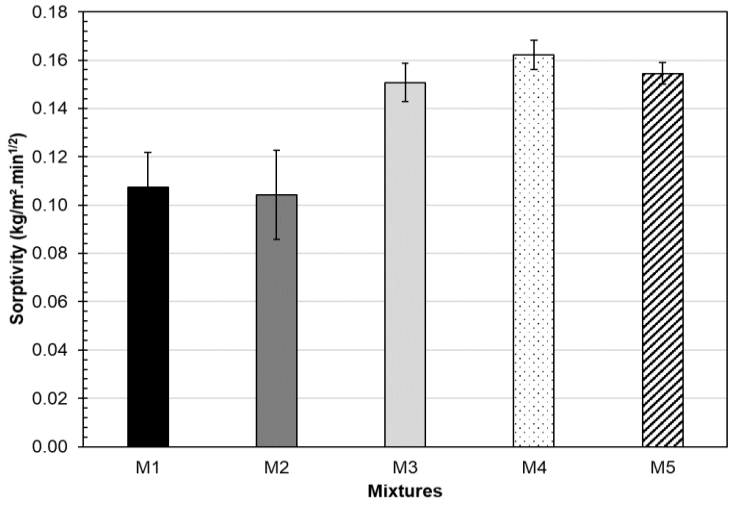

It is likely that mixtures M1 and M2 exhibited smaller amounts of capillary voids owing to the fact that they reached a higher temperature than the others, with greater evaporation of water and, consequently, reducing the amount of water present in the mortars. The water added to the geopolymer mixture has the main function of promoting fluidity and serving as the medium for the reactions, being evaporated after geopolymerization reactions [49]. Thus, a smaller quantity of water present in the mortar implies a lower number of voids and, therefore, less capillary absorption. Moreover, higher temperatures are conducive for the formation of a greater number of geopolymeric products, which fill voids and reduces the number of capillary pores [38, 39].

3.4.2 Shrinkage

Figure 9 illustrates the shrinkage results for the samples obtained from the five mixing routines. All mortars exhibited high shrinkage values (between 0.012% and 0.016%), stabilizing only after 21 days of age.

Figure 9: Drying shrinkage of mortars over time.

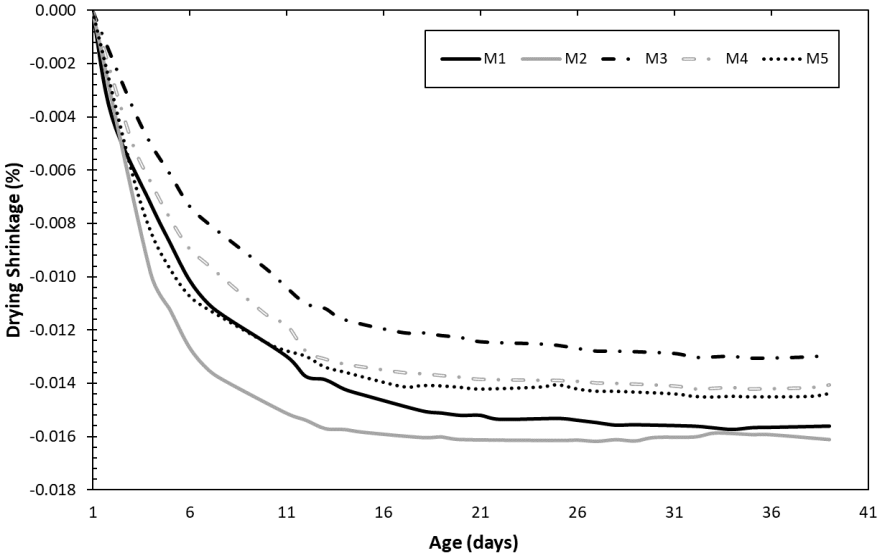

The mortars obtained from the M1 and M2 mixing routines exhibited higher shrinkage values, which is probably associated with the fact that these mixtures exhibited a high heat release, particularly in the initial moments (up to 20 h), as illustrated in Figure 4. Moreover, it was also observed that all the specimens suffered warping and cracking, as shown in Figure 10.

Figure 10: Specimens used for shrinkage evaluation, showing warping and cracking: (a) perspective view and (b) measurement of the inclination at the specimen end.

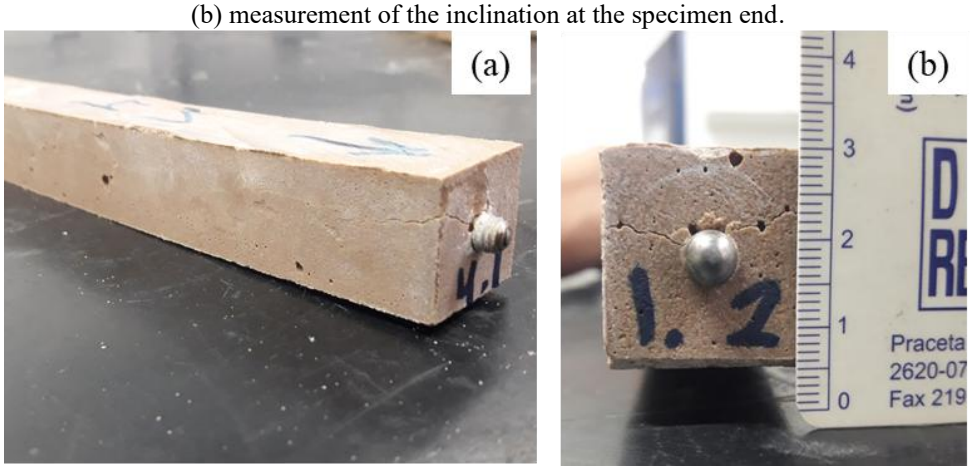

Figure 11 shows the results of the axial compressive strength of the samples obtained from the five mixing routines. At the initial ages, the M1 mixture exhibited superior mechanical performance, a phenomenon probably associated with the greater heat release observed in the calorimetry results (Figure 4). According to Eroshkina and Korovkin [50] and Cai et al. [2], temperature is a catalyst for geopolymeric reactions, influencing the greater dissolution of reactive components and the formation of reaction products.

There was also a loss of mechanical strength after 28 days of molding, which was observed in all mixtures. This phenomenon can be attributed to the development of cracks in the polymeric gel (Figure 11), caused by shrinkage due to water loss, or the occurrence of efflorescence [51, 52]. Considering that the formation of visible efflorescence was not identified in the studied artifacts, tests were performed to verify the shrinkage as a cause of the loss of strength after 28 days.

Figure 11: Evolution of the axial compressive strength of geopolymeric mortars for the five mixing procedures at the ages of 3, 7, and 28 days.

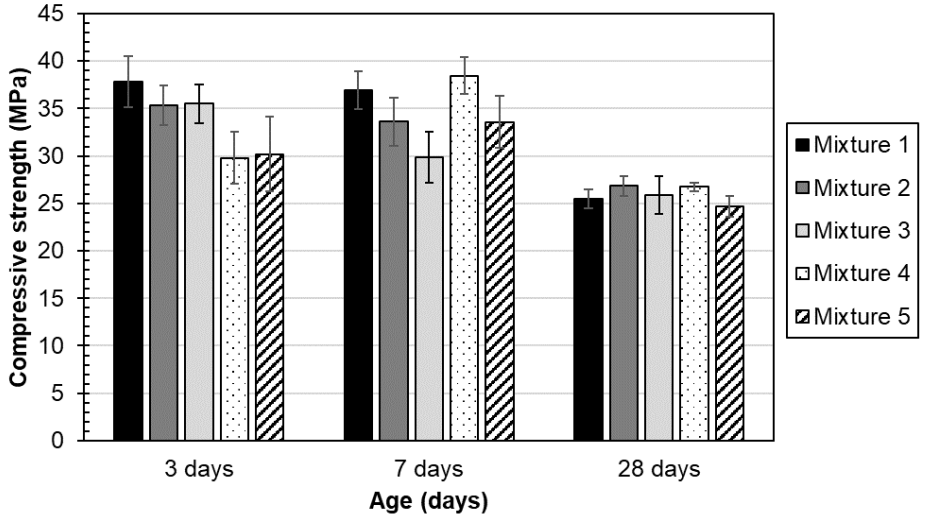

With the evolution from 3 days to 7 days, it was observed that the M1, M2, and M3 mixtures exhibited a loss of performance, unlike the M4 and M5 mixtures, which exhibited an increment in mechanical behavior. The behavior associated with M4 and M5 mixtures may be associated with greater solubilization of the silica present in sodium silicate because of its previous mixture with sodium hydroxide, making the development of geopolymeric compounds stand out for up to 7 days to shrinkage by drying. However, a reduction in mechanical strength was observed between 7 and 28 days, which normally occurs for geopolymer matrices that suffer excessive shrinkage [51, 52]. The effects of shrinkage, with the consequent appearance of cracks, are shown in Figure 12. Despite the difference in evolution, the mechanical strength results at 28 days of the mortars obtained by the different mixing methods did not show significant differences, which is evident in the ANOVA analysis (Table 4).

Figure 12: Cracks that occurred in the specimen of the M3 mixture after 7 days of age.

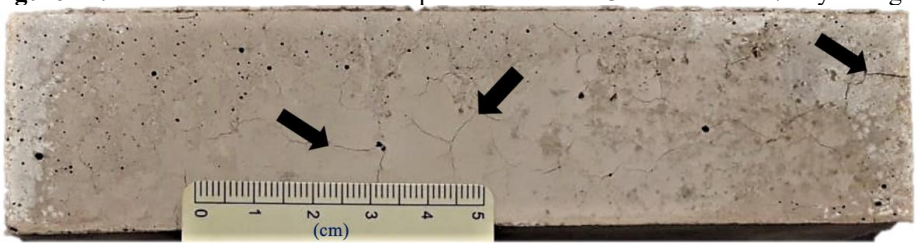

Table 4: Statistical reliability for the compressive strength test at 28 days, through analysis of variance (ANOVA).

Compressive strength	SQ	GL	MQ	F	p value	Fc	Significant Effect
Between Groups	12.03	4.00	3.01	2.78	0.07	3.11	No
Within groups	15.28	14.00	1.09				

Note: SQ – Square sum; GL – Degrees of freedom; MQ – square average; F – Calculated value of F; p value – significance level; Fc – F critical; If $p < 5\%$ and $Fc < F$, the effect is significant, considering the 95% confidence interval.

3.5 CONSIDERATIONS FOR MIXING ROUTINES

Based on the results obtained for the different mixing routines presented in the previous sections, the mortars did not show any significant difference in relation to the compressive strength at 28 days. However, considering the fact that the preparation and use of mortar and concrete occur in large volumes, the use of routines M1 and M2 is not recommended, as they would raise the temperature of

the mixture, with a greater release of heat, increasing the probability of cracks due to shrinkage, impairing workability, and leading to flash-set [2]. Therefore, the conventional mixing routine (M3) and routines with small variations (M4 and M5) are considered to be the most suitable.

4 CONCLUSIONS

In this study, work was done to evaluate the influence of five different mixing sequences on the workability, phase formation, and physical-mechanical properties of geopolymeric mortars with metakaolin as a precursor. From the results presented, it is concluded that:

- Because of the greater number of cracks originating in the matrices produced with the M1 and M2 routines, resulting from the high drying shrinkage presented by the specimens, the different mixing procedures did not significantly influence the compressive strength of geopolymeric mortars.
- The one-part procedure (M1) used in this work does not seem to be the most suitable for the production of high quantities of geopolymeric mortars/concretes, owing to the higher heat released and consequent losses of workability and shrinkage.
- According to the FTIR and calorimetry analyses, the M1 and M2 mixtures exhibited greater geopolymerization synthesis, most likely promoting greater densification of these matrices.
- The conventional two-part mixing procedure (M3) and its variables (M4 and M5) exhibited similar results in the fresh and hardened states, in addition to exhibiting lower shrinkage and released heat, which is the most suitable for the production of geopolymeric binders.

REFERENCES

[1] N. S. Amorim Júnior, J. S. A. Neto, H. A. Santana, M. S. Cilla, D. V. Ribeiro, “Durability and service life analysis of metakaolin-based geopolymer concretes with respect to chloride penetration using chloride migration test and corrosion potential,” *Construction and Building Materials*, vol. 287, p. 122970, 2021.

[2] J. Cai, X. Li, J. Tan, B. Vandevyvere, “Fly ash-based geopolymer with self-heating capacity for accelerated curing,” *Journal of Cleaner Production*, vol. 261, p. 121119, 2020.

[3] A. S. Ruviaro, H. A. Santana, G. T. dos Santos Lima, M. T. Barraza, L. Silvestro, P. J. P. Gleize, F. Pelisser, “Valorization of oat husk ash in metakaolin-based geopolymer pastes,” *Construction and Building Materials*, vol. 367, p. 130341, 2023.

[4] N. Ye, J. Yang, S. Liang, Y. Hu, J. Hu, B. Xiao, Q. Huang, “Synthesis and strength optimization of one-part geopolymer based on red mud,” *Construction and Building Materials*, vol. 111, pp. 317–325, 2016.

[5] Y. Aygörmez, O. Canpolat, M. M. Al-Mashhadani, “Assessment of geopolymer composites durability at one year age,” *Journal of Building Engineering*, vol. 32, p. 101453, 2020.

[6] H. A. Santana, N. S. A. Júnior, G. O. Carneiro, D. V. Ribeiro, M. S. Cilla, C. M. Dias, “Asbestos-cement wastes as supplementary precursors of NaOH-activated binders,” *Construction and Building Materials*, vol. 364, p. 129921, 2023.

[7] H. A. Santana, N. S. A. Júnior, D. V. Ribeiro, M. S. Cilla, C. M. Dias, “Vegetable fibers behavior in geopolymers and alkali-activated cement based matrices: A review,” *Journal of Building Engineering*, vol. 44, p. 103291, 2021.

[8] G. Mathew, B. M. Issac, “Effect of molarity of sodium hydroxide on the aluminosilicate content in laterite aggregate of laterised geopolymer concrete,” *Journal of Building Engineering*, vol. in press, p. 101486, 2020.

[9] P. Zhang, Z. Gao, J. Wang, J. Guo, S. Hu, Y. Ling, “Properties of fresh and hardened fly ash/slag based geopolymer concrete: A review,” *Journal of Cleaner Production*, vol. 270, p. 122389, 2020.

[10] J. Davidovits, *Geopolymer Chemistry and Applications*. Institut Géopolymère, 2011.

[11] R. Chen, S. Ahmari, L. Zhang, “Utilization of sweet sorghum fiber to reinforce fly ash-based geopolymer,” *Journal of Materials Science*, vol. 49, no. 6, pp. 2548–2558, 2014.

[12] T. Phoo-Ngernkham, A. Maegawa, N. Mishima, S. Hatanaka, P. Chindaprasirt, “Effects of sodium hydroxide and sodium silicate solutions on compressive and shear bond strengths of FA–GBFS geopolymer,” *Construction and Building Materials*, vol. 91, pp. 1–8, 2015.

[13] H. A. Santana, J. S. Andrade Neto, N. S. Amorim Junior, D. V. Ribeiro, M. S. Cilla, C. M. R. Dias, “Self-compacting geopolymer mixture: Dosing based on statistical mixture design and simultaneous optimization,” *Construction and Building Materials*, vol. 249, p. 118677, 2020.

[14] L. N. Assi, K. Carter, E. Deaver, P. Ziehl, “Review of availability of source materials for geopolymer/sustainable concrete,” *Journal of Cleaner Production*, vol. 263, p. 121477, 2020.

[15] H. A. Santana, J. S. Andrade Neto, D. V. Ribeiro, M. S. Cilla, C. M. Dias, “Accelerated alkaline attack of 3D printing polymers to assess their durability in geopolymer-based matrices,” *Journal of Materials in Civil Engineering*, vol. 33, no. 11, p. 04021327, 2021.

[16] H. A. Santana, N. S. A. Júnior, D. V. Ribeiro, M. S. Cilla, C. M. Dias, “3D printed mesh reinforced geopolymer: Notched prism bending,” *Cement and Concrete Composites*, vol. 116, p. 103892, 2021.

[17] E. Luga, C. D. Atis, “Optimization of heat cured fly ash/slag blend geopolymer mortars designed by ‘Combined Design’ method: Part 1,” *Construction and Building Materials*, vol. 178, pp. 393–404, 2018.

[18] L. Yun-Ming, H. Cheng-Yong, L. Li, N. A. Jaya, M. M. A. B. Abdullah, T. S. Jin, K. Hussin, “Formation of one-part-mixing geopolymers and geopolymer ceramics from geopolymer powder,” *Construction and Building Materials*, vol. 156, pp. 9–18, 2017.

[19] J. B. M. Dassekpo, X. Zha, J. Zhan, J. Ning, "The effects of the sequential addition of synthesis parameters on the performance of alkali activated fly ash mortar," *Results in Physics*, vol. 7, pp. 1506–1512, 2017.
[20] G. Görhan, G. Kürklü, "The influence of the NaOH solution on the properties of the fly ash-based geopolymer mortar cured at different temperatures," *Composites Part B: Engineering*, vol. 58, pp. 371–377, 2014.
[21] S. H. Bong, B. Nematollahi, M. Xia, A. Nazari, J. Sanjayan, "Properties of one-part geopolymer incorporating wollastonite as partial replacement of geopolymer precursor or sand," *Materials Letters*, vol. 263, p. 127236, 2020.
[22] M. Askarian, Z. Tao, B. Samali, G. Adam, R. Shuaibu, "Mix composition and characterisation of one-part geopolymers with different activators," *Construction and Building Materials*, vol. 225, pp. 526–537, 2019.
[23] B. Nematollahi, J. Sanjayan, F. U. A. Shaikh, "Synthesis of heat and ambient cured one-part geopolymer mixes with different grades of sodium silicate," *Ceramics International*, vol. 41, no. 4, pp. 5696–5704, 2015.
[24] M. X. Peng, Z. H. Wang, S. H. Shen, Q. G. Xiao, "Synthesis, characterization and mechanisms of one-part geopolymeric cement by calcining low-quality kaolin with alkali," *Materials and Structures*, vol. 48, pp. 699–708, 2015.
[25] M. I. A. Aleem, P. D. Arumairaj, "Geopolymer concrete – a review," *International Journal of Engineering Sciences & Emerging Technologies*, vol. 1, no. 2, pp. 118–122, 2012.
[26] A. Mehta, R. Siddique, "An overview of geopolymers derived from industrial by-products," *Construction and Building Materials*, vol. 127, pp. 183–198, 2016.
[27] Associação Brasileira de Normas Técnicas, "NBR 16916: Agregado miúdo – Determinação da densidade e da absorção de água," Rio de Janeiro, 2021.
[28] Associação Brasileira de Normas Técnicas, "NBR 17054: Agregados – Determinação da composição granulométrica – Método de ensaio," Rio de Janeiro, 2022.
[29] M. Lizcano, H. S. Kim, S. Basu, M. Radovic, "Mechanical properties of sodium and potassium activated metakaolin-based geopolymers," *Journal of Materials Science*, vol. 47, pp. 2607–2616, 2012.
[30] EFNARC, *Specification and Guidelines for Self-Compacting Concrete*. London, UK, 2002.
[31] EFNARC, *The European Guidelines for Self-Compacting Concrete*. 2005.
[32] Associação Brasileira de Normas Técnicas, "NBR 5738: Concreto – Procedimento para moldagem e cura de corpos de prova," Rio de Janeiro, 2016.
[33] Associação Brasileira de Normas Técnicas, "NBR 9779: Argamassa e concreto endurecidos – Determinação da absorção de água por capilaridade," Rio de Janeiro, 2012.
[34] Associação Brasileira de Normas Técnicas, "NBR 5739: Concreto – Ensaio de compressão de corpos-de-prova cilíndricos," Rio de Janeiro, 2018.
[35] J. L. Provis, P. Duxson, J. S. J. Van Deventer, "The role of particle technology in developing sustainable construction materials," *Advanced Powder Technology*, vol. 21, pp. 2–7, 2010.
[36] N. K. Lee, H. K. Lee, "Reactivity and reaction products of alkali-activated fly ash/slag paste," *Construction and Building Materials*, vol. 81, pp. 303–312, 2015.
[37] Y. Ling, K. Wang, X. Wang, S. Hua, "Effects of mix design parameters on heat of geopolymerization, set time, and compressive strength of high calcium fly ash geopolymer," *Construction and Building Materials*, vol. 228, p. 116763, 2019.
[38] J. Cai, X. Li, J. Tan, B. Vandevyvere, "Thermal and compressive behaviors of fly ash and metakaolin-based geopolymer," *Journal of Building Engineering*, vol. 30, p. 101307, 2020.
[39] Z. Hu, M. Wyrzykowski, P. Lura, "Estimation of reaction kinetics of geopolymers at early ages," *Cement and Concrete Research*, vol. 129, p. 105971, 2020.
[40] A. Allahverdi, E. Najafi Kani, "Construction wastes as raw materials for geopolymer binders," *International Journal of Civil Engineering*, vol. 7, no. 3, pp. 154–160, 2009.
[41] A. Kumar, S. Kumar, "Development of paving blocks from synergistic use of red mud and fly ash using geopolymerization," *Construction and Building Materials*, vol. 38, pp. 865–871, 2013.
[42] C. A. Rosas-Casarez et al., "Experimental study of XRD, FTIR and TGA techniques in geopolymeric materials," *International Journal of Advanced Computer Science*, vol. 4, pp. 221–226, 2014.
[43] E. Álvarez-Ayuso et al., "Environmental, physical and structural characterisation of geopolymer matrixes synthesised from coal (co-) combustion fly ashes," *Journal of Hazardous Materials*, vol. 154, no. 1–3, pp. 175–183, 2008.
[44] Z. Zhang, H. Wang, J. L. Provis, "Quantitative study of the reactivity of fly ash in geopolymerization by FTIR," *Journal of Sustainable Cement-Based Materials*, vol. 1, no. 4, pp. 154–166, 2012.
[45] T. Bakharev, "Geopolymeric materials prepared using Class F fly ash and elevated temperature curing," *Cement and Concrete Research*, vol. 35, no. 6, pp. 1224–1232, 2005.
[46] E. A. S. Vassalo, *Obtenção de geopolímero a partir de metacaulim ativado*. Dissertação de mestrado, Belo Horizonte, 2013.
[47] S. Xu, M. A. Malik, Z. Qi, B. Huang, Q. Li, M. Sarkar, "Influence of the PVA fibers and SiO_2 NPs on the structural properties of fly ash based sustainable geopolymer," *Construction and Building Materials*, vol. 164, pp. 238–245, 2018.
[48] J. L. Provis, S. A. Bernal, "Geopolymers and related alkali-activated materials," *Annual Review of Materials Research*, vol. 44, pp. 299–327, 2014.
[49] P. Duxson et al., "Understanding the relationship between geopolymer composition, microstructure and mechanical properties," *Colloids and Surfaces A*, vol. 269, pp. 47–58, 2005.
[50] N. Eroshkina, M. Korovkin, "The effect of the mixture composition and curing conditions on the properties of the geopolymer binder based on dust crushing of the granite," *Procedia Engineering*, vol. 150, pp. 1605–1609, 2016.
[51] M. Ibrahim, M. A. M. Johari, M. K. Rahman, M. Maslehuddin, "Effect of alkaline activators and binder content on the properties of natural pozzolan-based alkali activated concrete," *Construction and Building Materials*, vol. 147, pp. 648–660, 2017.
[52] A. Wardhono, D. W. Law, T. C. K. Molyneaux, "Long term performance of alkali activated slag concrete," *Journal of Advanced Concrete Technology*, vol. 13, pp. 187–192, 2015.

Author Contributions: N. S. A. J.: Methodology, Investigation, Formal analysis, Data curation, Writing – original draft. **J. S. A. N.:** Methodology, Investigation, Formal analysis, Data curation, Writing – original draft. **H. A. S.:** Writing – review & editing, Validation, Methodology, Investigation, Formal analysis, Data curation, Conceptualization. **M. S. C.:** Supervision, Methodology, Funding acquisition, Data curation, Writing – original draft. **D. V. R.:** Supervision, Methodology, Investigation, Funding acquisition, Formal analysis, Data curation.